Heterosupramolecular Chemistry: An Approach to Modulating Function in Molecular Devices

Xavier Marguerettaz, Gareth Redmond, S. Nagaraja Rao, and Donald Fitzmaurice*

Abstract: Linked viologen–anthraquinone molecules are attached to TiO_2 nanocrystallites supported on a conducting glass substrate. The resulting assembly is incorporated as the working electrode in an electrochemical cell. Under open-circuit conditions, band-gap excitation of the semiconductor nanocrystallite results in viologen-mediated electron transfer to anthraquinone. Prior application of a negative potential step, which results in $2e^-/2H^+$ reduction of anthraquinone, permits electron transfer only to viologen. At positive applied potentials, electron transfer following band-gap excitation is largely suppressed. Some implications of these findings for modulation of function in molecular devices are considered.

Keywords
anthraquinones · molecular devices · supramolecular chemistry · titanium dioxide · viologens

Introduction

Supramolecular chemistry is distinguished from large-molecule chemistry[1, 2] by the the fact that the intrinsic properties of the molecular components are only slightly perturbed within the supermolecule, and the properties of the supermolecule are not a simple superposition of the properties of the molecular components (i.e., there exists a supramolecular function). Another important aspect of supramolecular chemistry is the organisation of supermolecules and consequent addressability of function.

Addressable supramolecular function offers the prospect of constructing molecular devices.[3–5] The constituent supramolecular entities may be photo-, electro-, iono-, magneto-, thermo-, mechano- or chemoactive, depending on whether they process photons, electrons or ions, respond to magnetic fields or to heat, undergo changes in mechanical properties or perform a chemical reaction. However, despite many beautiful examples of organised supramolecular assemblies, progress toward realisation of practical molecular devices has, in fact, been slow.

The reasons for the limited progress to date are linked to the stringent requirements that must be met by practical devices: firstly, that they function at a supramolecular level within an organised assembly; secondly, that the function of each constituent supermolecule in a given assembly can be modulated independently; thirdly, that the state of modulation of each supermolecule in a given assembly can be determined individually; and finally, that the resulting device meet speed, reliability and cost specifications.

[*] D. Fitzmaurice, X. Marguerettaz, G. Redmond, S. N. Rao
Department of Chemistry, University College Dublin
Dublin 4 (Ireland)
Fax: Int. code +(1)283-7873
e-mail: donfitzm@irlearn.ucd.ie

In practice, problems encountered include:[1–5] firstly, constituent supramolecular units do not act independently; secondly, attempts to modulate supramolecular function typically involve incorporation of subunits within a supermolecule that respond to external stimuli, an approach which to date has produced relatively small effects; thirdly, substrates supporting an organised assembly that are capable of affecting the stimulus of the above subunits and providing information concerning their modulation state have proved difficult to identify; finally, techniques that permit the constituent supermolecules of the molecular device to be addressed individually have not yet been realised, although recent progress is encouraging.[6]

Regarding substrates that are capable of modulating supramolecular function and providing information concerning modulation state, heterosupramolecular chemistry may offer new opportunities.[7, 8]

By replacing a molecular component in a supermolecule by a condensed-phase component, referred to as a heterocomponent, a heterosupermolecule is formed. By analogy with supramolecular chemistry, the properties of the heterosupermolecule are not a simple superposition of the properties of the heterocomponent and molecular components (i.e., there exists a heterosupramolecular function). As for supermolecules, addressability is a consequence of organisation. Uniquely, however, because the assembled heterosupermolecules possess a condensed-phase component, organisation may yield an intrinsic substrate capable of modulating function within the constituent heterosupermolecules and providing information concerning their modulation state.

Here, we report results for a heterosupramolecular assembly in which linked viologen–anthraquinone molecules are attached to TiO_2 nanocrystallites supported on a conducting glass substrate. The resulting assembly is incorporated as the working electrode in an electrochemical cell. Under open-circuit conditions, band-gap excitation of the semiconductor nanocrystallite results in viologen-mediated electron transfer to anthraquinone.

0947-6539/96/0204-0420 $ 15.00+.25/0

Prior application of a negative potential step, which results in $2e^-/2H^+$ reduction of anthraquinone, permits electron transfer only to viologen. At positive applied potentials, electron transfer following band-gap excitation is largely suppressed. Some implications of these findings for modulation of function in molecular devices are considered.

Results and Discussion

Characterisation of Heterosupramolecular Assemblies: TiO_2 nanocrystallites, when deposited on conducting glass and fired, yield a transparent nanocrystalline semiconductor substrate in ohmic contact with the conducting support. Consequently, following incorporation as the working electrode of an electrochemical cell, potentiostatic control of the quasi-Fermi level within the substrate is possible.[9] At applied potentials more negative than that of the conduction band edge at the semiconductor–liquid electrolyte solution interface (V_{cb}), electrons are accumulated in the available states of the conduction band. By examining the dependence on potential of the optical absorption assigned to such electrons, it is possible to determine V_{cb}. Further, V_{cb} exhibits the expected pH dependence, shifting to more negative potentials by 0.060 V per pH unit [Eq. (1)].

$$V_{cb} = -0.40 - 0.060\,pH\ (V, SCE) \quad (1)$$

It has been shown that molecules such as salicylic acid are strongly chemisorbed at TiO_2.[10, 11] Therefore, this and related molecules are used to attach previously linked molecular components to the surface of the nanocrystallites of the semiconductor substrate. Adsorption is monitored spectroscopically by means of a visible charge-transfer absorption assigned to salicylic acid and related molecules chemisorbed at TiO_2.[10, 11] It has been proposed that salicylic acid is chemisorbed by chelation to surface Ti^{4+} atoms.[10, 11] The surface density of such sites has been determined to be 2×10^{13} cm^{-2}.[12] The molecular components S, SV, SVQ and SQ examined in this paper are shown in Scheme 1. The heterosupramolecular assemblies formed by linkage to nanocrystalline TiO_2 substrates are denoted $H(TiO_2)$–S, $H(TiO_2)$–SV, $H(TiO_2)$–SVQ and $H(TiO_2)$–SQ, respectively.

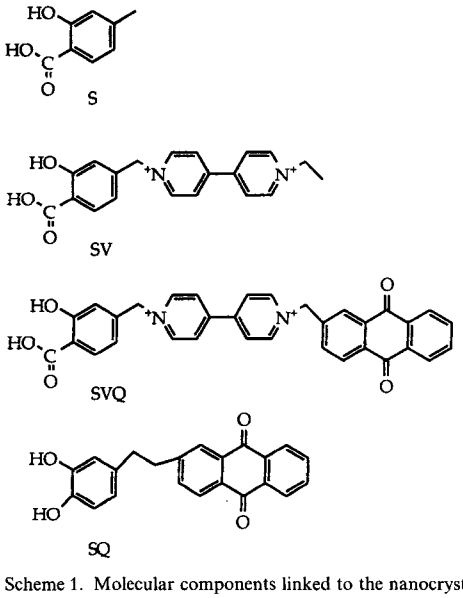

Scheme 1. Molecular components linked to the nanocrystalline TiO_2 substrate.

Potential-Induced Vectorial Electron Flow in $H(TiO_2)$–SVQ: Recently, potential-induced vectorial electron flow in $H(TiO_2)$–SVQ at applied potentials more negative than V_{cb} has been reported (Scheme 2).[8] These findings are summarised briefly.

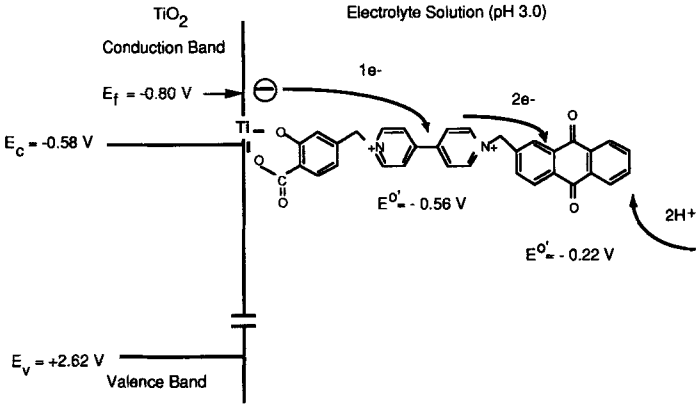

Scheme 2. Potential-induced vectorial electron flow in $H(TiO_2)$–SVQ.

The first cathodic scan of a cyclic voltammogram (CV) recorded at pH 3.0 for $H(TiO_2)$–SVQ shows a wave at -0.6 V due to $1e^-$ reduction of viologen and $2e^-/2H^+$ viologen-mediated reduction of anthraquinone (Fig. 1a).[8] The first anodic scan shows a wave at -0.5 V, the result of $1e^-$ oxidation of

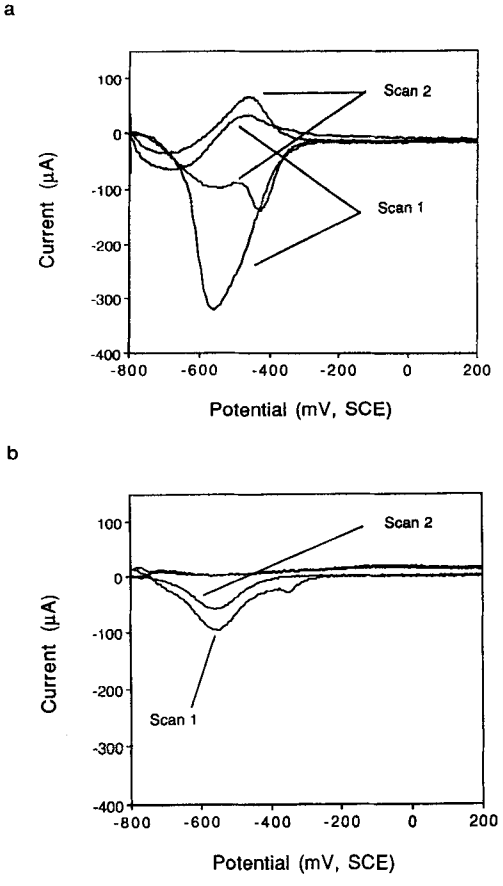

Fig. 1. Cyclic voltammograms recorded for a) $H(TiO_2)$–SVQ (SVQ adsorbed during 30 min from a 1×10^{-3} mol dm^{-3} aqueous solution) and b) $H(TiO_2)$–SQ (SQ adsorbed during 30 min from a 2×10^{-3} mol dm^{-3} aqueous solution). A deaerated aqueous electrolyte was used (pH = 3) and the voltammogram for bare TiO_2 substrate subtracted (see Experimental Procedure for details).

viologen. Subsequent cathodic scans continue to show a wave at -0.6 V due to reduction of viologen, although no current due to viologen-mediated reduction of anthraquinone is observed. Subsequent anodic scans show a wave at -0.5 V due to $1e^-$ oxidation of viologen and are similar to the initial anodic scan. Analysis of the CVs in Figure 1a indicates the integrated cathodic current due to direct reduction of viologen is about 40% of that due to viologen-mediated reduction of anthraquinone, that is, close to the expected value of 33%. It is estimated, therefore, that reduction of anthraquinone is 90% viologen-mediated. When air is bubbled through the electrolyte for 20 min at the rest potential of $+0.20$ V, anthraquinone is regenerated and CVs similar to those initially observed are recorded. The CVs shown in Figure 1a are typical of many such experiments and consistent with previously reported CVs for polymeric viologens charge-compensated by anthraquinone.[13, 14]

An alternative explanation that would also be consistent with the CVs shown in Figure 1a is that viologen and anthraquinone are directly reduced on the first cathodic scan and that only viologen is reoxidised on the first and subsequent anodic scans. Specifically, on the second and subsequent cathodic scans only reduction of viologen would be observed. However, this possibility may be excluded on the basis of CVs recorded for the model compound $H(TiO_2)$–SQ (Fig. 1b). On the first cathodic scan the peak reduction current is observed at about -0.6 V, consistent with a value of V_{cb} of -0.58 V in aqueous solution at pH 3.0. The formal potential for anthraquinone in aqueous solution at pH 3.0 is estimated to be -0.2 V.[15] On the first anodic scan significant reoxidation is observed, and the second cathodic scan consequently yields an integrated current in good agreement with that measured for the first cathodic scan. We note that the difference between the first and second cathodic scans is largely accounted for by deep-trap filling in the semiconductor electrode. These results demonstrate that anthraquinone molecules reduced directly at the semiconductor electrode are also reoxidised.[13, 14] This, in turn, supports the interpretation of the loss of cathodic current in Figure 1a as being due to viologen-mediated reduction of anthraquinone.

A series of visible absorption spectra were also measured for $H(TiO_2)$–SVQ between 0.00 V and -0.80 V (Fig. 2a). At applied potentials more negative than -0.4 V, but more positive than V_{cb}, an absorbance spectrum assigned to reduced anthraquinone (i.e., dihydroanthraquinone) is observed.[16] The measured spectrum necessarily corresponds to that of anthraquinone molecules reduced directly at the semiconductor electrode, since the applied potentials is not sufficiently negative to reduce viologen. More quantitatively, the measured spectra indicate that about 15% of anthraquinone molecules are reduced directly at the TiO_2 substrate. At potentials more negative than V_{cb}, a spectrum, which may be assigned to the summed spectra of reduced viologen and anthraquinone, is measured.[16–19] Further, as can be seen from Figure 2b, the contribution by reduced anthraquinone to a spectrum measured at -0.40 V and -0.50 V is significantly greater for the reverse potential sweep. Thus, the remaining anthraquinone molecules are reduced only at potentials sufficiently negative to reduce viologen. The observed potential-dependent spectra are therefore consistent with viologen-mediated reduction of anthraquinone. Finally, we note that at 0.00 V the spectrum assigned to reduced anthraquinone persists for up to 5 min; this suggests long-lived charge trapping. The reduced anthraquinone is oxidised by reaction with residual dissolved molecular oxygen, which is transformed to peroxide.[20] The final spectrum is indistinguishable from that measured initially at 0.00 V.

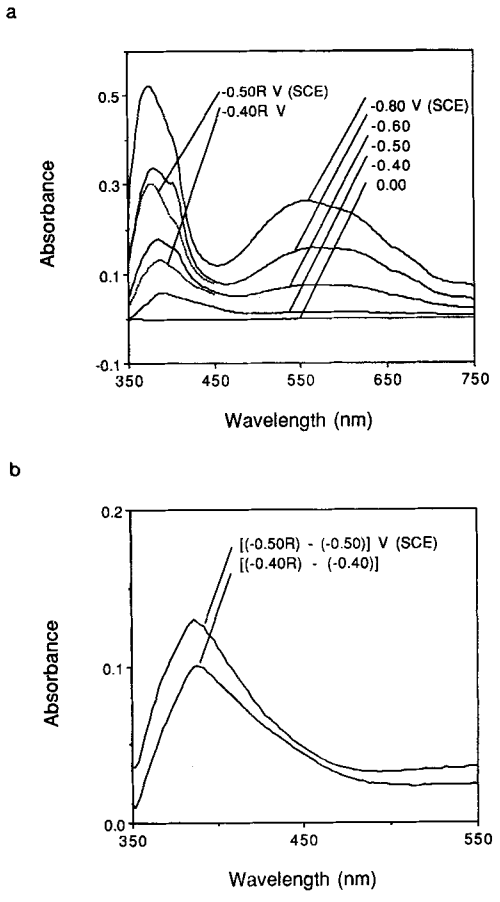

Fig. 2. a) Absorbance spectra of $H(TiO_2)$–SVQ (SVQ adsorbed during 60 min from a 1×10^{-3} mol dm^{-3} aqueous solution) at applied potentials between 0.00 and -0.80 V (aqueous electrolyte, pH = 3; see Experimental Procedure for details). b) Difference between the absorbance spectra in a) measured at -0.40 and -0.50 V on changing the applied potential first in the cathodic and then in the anodic directions.

Light-Induced Vectorial Electron Flow in $H(TiO_2)$–SVQ: Based on the findings outlined above, it was expected that band-gap irradiation of $H(TiO_2)$–SVQ would result in viologen-mediated electron transfer to anthraquinone. Further, it was expected that the reduced anthraquinone would add hydrogen and long-lived charge-trapping result (Scheme 3).

To test these predictions, $H(TiO_2)$–SVQ was placed in a deaerated acidified ethanolic solution (pH 3.0) and irradiated from the conducting glass side at 355 nm for 60 s with the pulsed

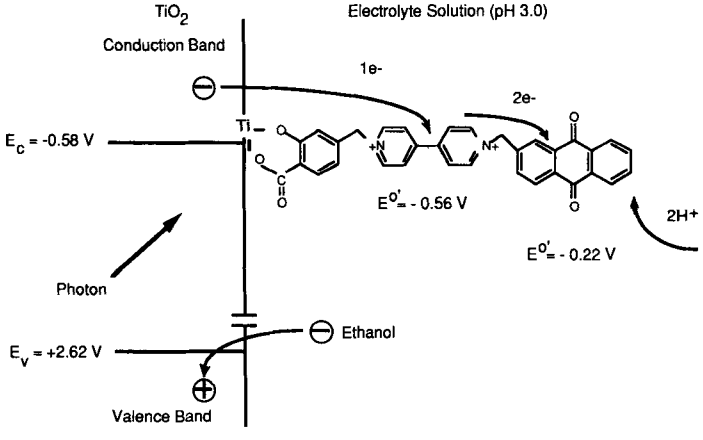

Scheme 3. Light-induced vectorial electron flow in $H(TiO_2)$–SVQ.

0947-6539/96/0204-0422 $ 15.00+.25/0 Chem. Eur. J. 1996, 2, No. 4

output of a frequency-tripled Nd:Yag laser.[21] Following irradiation, the measured visible absorption spectrum was principally that of reduced viologen[16–18] and reduced anthraquinone (Fig. 3a).[18] An ethanolic solution was used to ensure efficient trapping of photogenerated holes and electron transfer to the viologen.[22] The same experiment performed in aqueous electrolyte solution produced no detectable concentration of reduced viologen or reduced anthraquinone. The decay of reduced viologen and anthraquinone was monitored by recording spectra at 60 s intervals (Fig. 3a). The absorbance

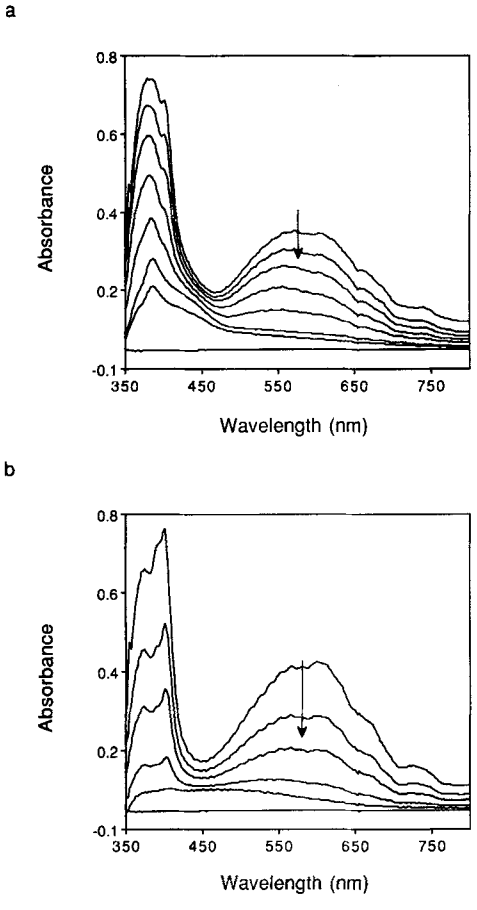

Fig. 3. Absorbance spectra following pulsed irradiation for 60 s with the frequency-tripled output (355 nm) of a Nd:Yag laser (10 Hz, 4.3 mJ pulse^{-1}): a) H(TiO_2)–SVQ (SVQ adsorbed during 60 min from a 1×10^{-3} mol dm^{-3} aqueous solution), measured at 60 s intervals; and b) H(TiO_2)–SV (SV adsorbed during 60 min from a 2×10^{-3} mol dm^{-3} aqueous solution), measured at 40 s intervals. A deaerated, acidified ethanolic electrolyte was used (see Experimental Procedure for details). Also shown are the baseline absorbances recorded prior to irradiation.

assigned to reduced viologen decays completely in about 5 min, presumably, by reaction with residual oxygen; however, the possibility of electron transfer by reduced viologen to surface states on the semiconductor substrate or to reoxidised anthraquinone cannot be excluded. The spectrum assigned to reduced anthraquinone is then apparent and decays in about 12 min by reaction with residual oxygen to form peroxide.[20]

Spectra measured for H(TiO_2)–SV under similar conditions are entirely consistent with the above findings (Fig. 3b). Briefly, for H(TiO_2)–SV the spectrum observed following irradiation was that of reduced viologen and decays over about 5 min. No long-lived residual absorbance, such as that assigned to reduced anthraquinone in Figure 3a, is observed. In turn, this suggests decay of reduced viologen in H(TiO_2)–SVQ by electron transfer to reoxidised anthraquinone is not important.

A series of CV experiments for H(TiO_2)–SVQ in a deaerated and acidified ethanolic solution (pH 3.0) were also performed, following 10 min irradiation with the frequency-tripled output (355 nm) of a Nd:Yag laser (Fig. 4a). No current is observed during the first cathodic scan that could be assigned to viologen-mediated reduction of anthraquinone. It is concluded that light-induced vectorial electron flow has previously reduced anthraquinone. This is consistent with the fact that, following irradiation under similar conditions, the measured absorbance spectrum is that of reduced viologen and reduced anthraquinone (Fig. 3a). This interpretation is further supported by the fact that the regeneration of anthraquinone in situ, by first bubbling air through the electrolyte for 20 min and then argon for 30 min, results in the CVs shown in Figure 4b. Specifically, during the next cathodic scan, current that can be assigned to viologen-mediated reduction of anthraquinone is observed and is absent in subsequent cathodic scans.

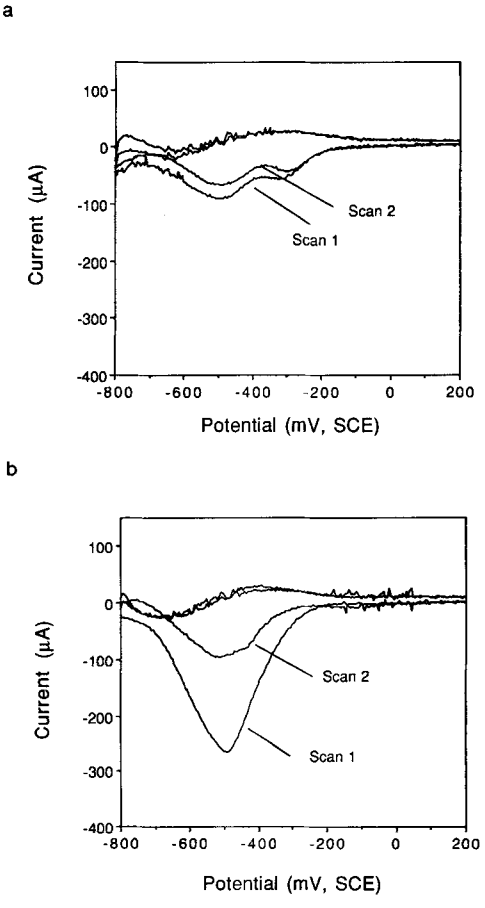

Fig. 4. a) Cyclic voltammogram, following 10 min irradiation by the frequency-tripled output (355 nm) of a Nd:Yag laser (10 Hz, 2.0 mJ pulse^{-1}), of H(TiO_2)–SVQ (SVQ adsorbed during 30 min from a 1×10^{-3} mol dm^{-3} aqueous solution) in a deaerated, acidified ethanolic electrolyte (see Experimental Procedure for details). b) Cyclic voltammogram of substrate in a) after bubbling air through the electrolyte for 20 min and then argon for 30 min. The background voltammogram measured for the bare TiO_2 substrate has been subtracted in a) and b).

Based on the above results it may be concluded that 1) band-gap excitation does lead to formation of reduced viologen and reduced anthraquinone, and 2) following electron transfer to anthraquinone protonation results in long-lived charge trapping. Based on the results presented for potential-induced reduction in H(TiO_2)–SVQ, we assume also that electron transfer to anthraquinone is viologen-mediated. Below we discuss kinet-

ic evidence that further supports this assertion and permits a mechanism to be proposed.

Kinetics of Light-Induced Vectorial Electron Flow in $H(TiO_2)$–SVQ: As reoxidation of $H(TiO_2)$–SVQ is incomplete in the 0.1 s interval between 355 nm pulses, prolonged irradiation leads to accumulation of reduced viologen and anthraquinone and a corresponding increase in the measured absorbances at 400 and 600 nm (Fig. 5a). Significantly, at short times, absorbance growth is sigmoidal. The spectra shown in Figure 3, allow the absorbances at 400 nm and 600 nm to be assigned to reduced viologen and anthraquinone.

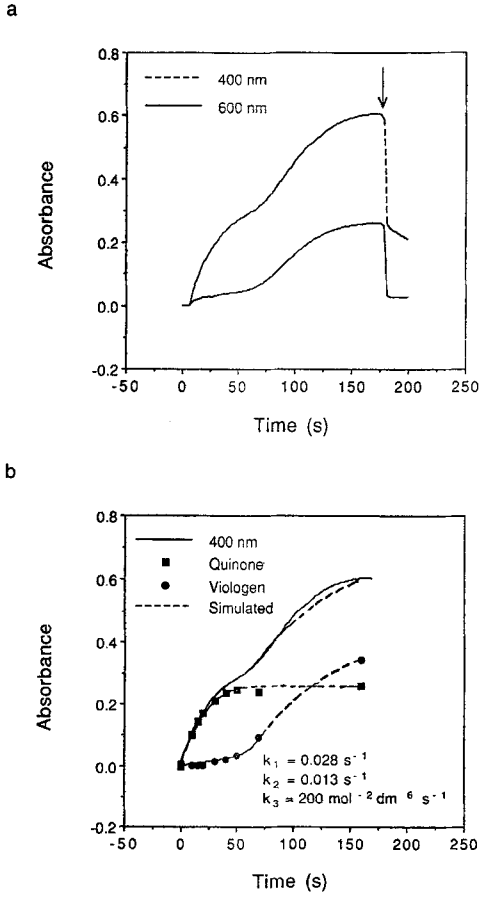

Fig. 5. a) Evolution of absorbance at 400 and 600 nm for $H(TiO_2)$–SVQ during pulsed irradiation by the frequency-tripled output (355 nm) of a Nd:Yag laser (10 Hz, 4.3 mJ pulse^{-1}). Conditions are as in Figure 3a. The arrow indicates the point at which irradiation was stopped and a positive potential (0.00 V) applied. b) The experimentally determined relative contributions to the absorbance measured at 400 nm (Fig. 5a) by reduced viologen and anthraquinone, and the predicted absorbances based on Equations (2) to (4).

To quantify the relative contributions to the absorbance measured at 400 nm by reduced viologen and anthraquinone the following approach was adopted: Irradiation was stopped and a positive potential (0.00 V) applied. This resulted in complete reoxidation of reduced viologen within 1 s. Accordingly, there is complete loss of absorbance at 600 nm (Fig. 5a). Similarly, the initial absorbance loss at 400 nm is assigned to reoxidation of reduced viologen. The residual absorbance at the same wavelength is, therefore, assigned to reduced anthraquinone. A series of experiments of this type were performed, and the results are summarised in Figure 5b.

It is evident from Figure 5b that only after all $SV^{2+}Q$ has been reduced to $SV^{2+}QH_2$ is $SV^{\bullet+}QH_2$ accumulated. It is proposed that the competing process is electron transfer from $SV^{\bullet+}QH_2$ to adjacent $SV^{2+}Q$. The reactions (2)–(4) are therefore proposed. Values for k_1 (0.028 s^{-1}), k_2 (0.035 s^{-1}) and k_3 (200 mol^{-2} dm^6 s^{-1}) were determined by fitting the absorbance measured at 400 nm (Fig. 5b). These rate constants were, in turn, used to predict the measured absorbance by reduced viologen and anthraquinone at 400 nm. The excellent agreement observed strongly supports the proposed mechanism.

$$SV^{2+}Q \xrightarrow{k_1} SV^{2+}QH_2 \quad (2)$$

$$SV^{2+}QH_2 \xrightarrow{k_2} SV^{\bullet+}QH_2 \quad (3)$$

$$SV^{2+}Q + 2SV^{\bullet+}QH_2 \xrightarrow{k_3} 3SV^{2+}QH_2 \quad (4)$$

A similar kinetic study was performed at 600 nm for $H(TiO_2)$–SV (Fig. 6a). An appropriate reaction scheme, consistent with that for $H(TiO_2)$–SVQ above, is given by Equation (5). The rate constant for formation of reduced viologen

$$SV^{2+} \xrightarrow{k'_1} SV^{\bullet+} \quad (5)$$

k'_1 (0.020 s^{-1}) could be determined by a fit to the absorbance data measured at 600 nm, and was, in turn, used to predict the

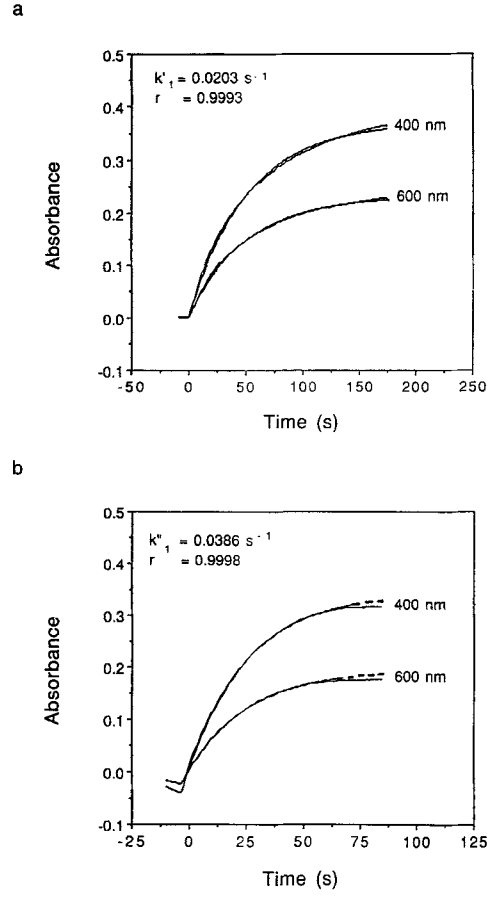

Fig. 6. a) Evolution of absorbance at 400 nm and 600 nm for $H(TiO_2)$–SV during pulsed irradiation by the frequency-tripled output (355 nm) of a Nd:Yag laser (10 Hz, 4.3 mJ pulse^{-1}). Conditions are as in Figure 3b. The predicted absorbances based on Equation (5) are also plotted and are almost superimposable on the experimental plots. b) Evolution of absorbance at 400 nm and 600 nm for $H(TiO_2)$–SVQ potentiostatically reduced to $SVQH_2$ during pulsed irradiation by the frequency-tripled output (355 nm) of a Nd:Yag laser (10 Hz, 4.3 mJ pulse^{-1}). Conditions are as in Figure 3a. Dashed line: predicted absorbance based on Equation (6).

0947-6539/96/0204-0424 $ 15.00+.25/0 Chem. Eur. J. 1996, 2, No. 4

measured absorbance at 600 nm (Fig. 6a); the agreement is excellent.

Finally, a kinetic study was performed at 600 nm for $H(TiO_2)$–SVQ following potentiostatic reduction of the anthraquinone component (Fig. 6b). An appropriate reaction scheme, consistent with that for $H(TiO_2)$–SVQ above, is given by Equation (6). The rate constant for formation of reduced

$$SV^{2+}QH_2 \xrightarrow{k_1''} SV^{\bullet+}QH_2 \quad (6)$$

viologen k_1'' ($0.038\ s^{-1}$) could be determined by a fit to the absorbance data measured at 600 nm, and was used to predict the measured absorbance at 600 nm (Fig. 6b); agreement is excellent. As expected, growth of the absorbance assigned to reduced viologen is no longer sigmoidal.

Comparing the resulting rate constants in Figures 5 and 6 for $H(TiO_2)$–SVQ and $H(TiO_2)$–$SVQH_2$, it is gratifying that the values determined for k_2 and k_1'' are similar, as they describe closely related processes. The difference observed is likely to be a consequence of irreversible occupation of deep-trap states during the negative potential step used to reduce $H(TiO_2)$–SVQ to $H(TiO_2)$–$SVQH_2$.

The above studies have established the principal features of a kinetic model for light-induced vectorial electron flow in $H(TiO_2)$–SVQ. Importantly, in order to account for the observed kinetic behaviour it has been necessary to include electron transfer from $SV^{\bullet+}QH_2$ to $SV^{2+}Q$, sometimes referred to as cross-talk. While this represents a limitation of the present system, it does nevertheless support the assertion that electron transfer to anthraquinone is viologen-mediated. Further, the proposed mechanism is consistent with the kinetic behaviour observed in the related systems, $H(TiO_2)$–SV and $H(TiO_2)$–$SVQH_2$, and with the findings of kinetic studies for related molecular diads and triads in solution.[23, 24] Future work will involve the use of sub-ps transient absorption spectroscopy to resolve the real-time rise of the transients assigned to reduced viologen and reduced anthraquinone. Such studies will be undertaken for analogous systems prepared using Langmuir–Blodgett techniques in which cross-talk is expected to be largely eliminated.

Finally, we note that in the course of the above discussion it has been assumed that reduction of anthraquinone is by a sequential $2e^-/2H^+$ process. The possibility that disproportionation of $H(TiO_2)$–SVQH results in formation of $H(TiO_2)$–$SVQH_2$ cannot be excluded. However, we also note, that such a reaction would not be inconsistent with a principal conclusion of this study, namely, that reduction of anthraquinone is viologen-mediated.

Modulation of Light-Induced Vectorial Electron Flow in $H(TiO_2)$–SVQ: As discussed above, vectorial electron flow in $H(TiO_2)$–SVQ may be initiated by band-gap excitation of the constituent semiconductor nanocrystallites, or potentiostatically by applying a potential more negative than V_{cb}.[8] The question then arises whether it is possible to modulate light-induced vectorial electron flow by controlling potentiostatically the energy of the quasi-Fermi level in the constituent nanocrystallites of $H(TiO_2)$–SVQ. The results of some initial experiments to test this possibility are discussed below.

$H(TiO_2)$–SVQ, forming the working electrode of an electrochemical cell containing acidified ethanolic electrolyte solution (pH 3.0), was irradiated from the conducting glass side at 355 nm for 90 s at the potential indicated in Figure 7 with the pulsed output of a frequency-tripled Nd:Yag laser. The absorbance measured at 600 nm and assigned principally to reduced viologen is plotted against irradiation time for different applied potentials.

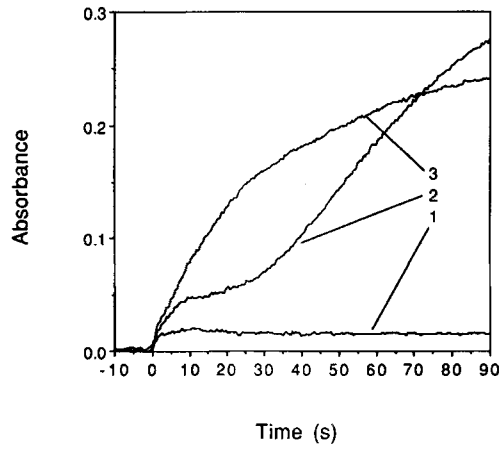

Fig. 7. Absorbance at 600 nm by $H(TiO_2)$–SVQ (SVQ adsorbed during 30 min from 1×10^{-3} mol dm^{-3} aqueous solution) in a deaerated, acidified ethanolic electrolyte (see Experimental Procedure for details) during irradiation by the frequency-tripled output (355 nm) of a Nd:Yag laser (10 Hz, 5.5 mJ $pulse^{-1}$). The applied potentials were 1) 0.70 V, 2) open circuit and 3) open circuit following application of a cathodic step from 0.00 to −0.70 V (60 s) returning to 0.00 V (15 s) prior to irradiation.

At the open-circuit potential (plot (2), Fig. 7) we observe sigmoidal growth of the absorbance at 600 nm assigned to reduced viologen. This behaviour is consistent with viologen-mediated reduction of anthraquinone (Fig. 5). Following application of a cathodic potential step between 0.00 and −0.70 V (60 s) and returning to 0.00 V (15 s) (plot (3), Fig. 7), formation of reduced viologen at the open-circuit potential is significantly faster and growth of the associated absorbance no longer sigmoidal. The increased rate of formation of reduced viologen is, as stated above, likely to be a consequence of irreversible occupation of electron-trap states during the negative potential step. The absence of the sigmoidal feature is consistent with prior reduction of anthraquinone. At an applied potential of 0.70 V (plot (1), Fig. 7) there is a small initial increase in absorbance by reduced viologen, but the steady-state value is significantly less than that measured at the open-circuit potential. This continues to be the case for the first few pulses, although continued irradiation results in accumulation of electrons in deep traps and a shift in the quasi-Fermi level to more negative potentials. As a consequence, the efficiency of interfacial electron transfer approaches that observed at the open-circuit potential. However, as the rate of reoxidation of reduced viologen is significantly faster at positive applied potentials, the reduced viologen generated by a single pulse is almost entirely reoxidised in the interval between successive pulses.

Similar experiments were performed with ns time resolution under single-shot conditions. The transient measured at the open-circuit potential (plot (2), Fig. 8a) is assigned to trapped electrons and to reduced viologen. The decay of this transient is assumed, on this timescale, to be due to electron transfer to anthraquinone. Support for this assertion is provided by measurement of a similar transient at the open-circuit potential following prior application of a cathodic potential step to reduce the anthraquinone (plot (3), Fig. 8a). Under these conditions virtually no decay of the absorbance assigned to reduced viologen is observed on the same timescale. The increased efficiency of formation of reduced viologen is, as above, attributed to deep-trap filling and a consequent shift to more negative potentials of the quasi-Fermi level. Finally, the transient measured under similar conditions at 0.70 V (plot (1), Fig. 8a) is assigned

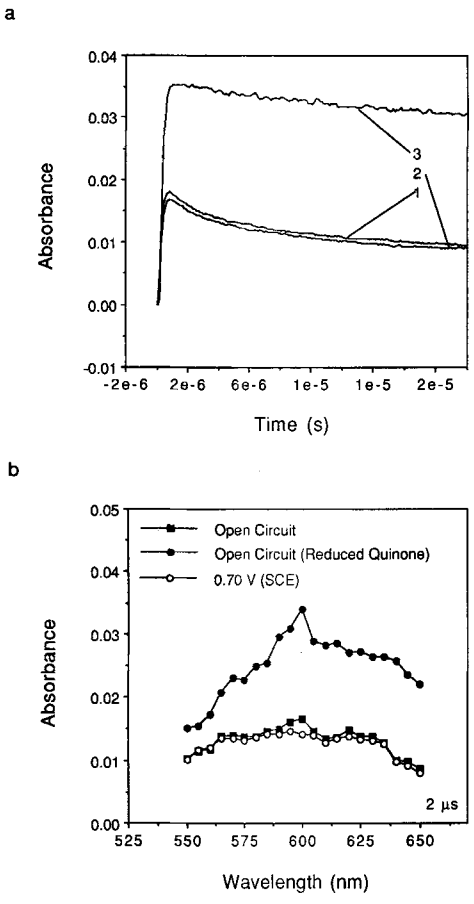

Fig. 8. a) Transient absorbance at 600 nm by $H(TiO_2)$–SVQ (SVQ adsorbed during 30 min from 1×10^{-3} mol dm^{-3} aqueous solution) in a deaerated, acidified ethanolic electrolyte (see Experimental Procedure for details) during irradiation by the frequency-tripled output (355 nm) of a Nd:Yag laser (10 Hz, 5.5 mJ pulse^{-1}). The applied potentials were 1) 0.70 V, 2) open circuit and 3) open circuit following application of a cathodic step from 0.00 to −0.70 V (60 s) returning to 0.00 V (15 s) prior to irradiation. b) Transient spectra measured after 2 μs at the indicated applied potentials.

principally to trapped electrons; a small residual absorbance by reduced viologen may also be present.

The above interpretation of the transients in Figure 8a is confirmed by examination of the transient spectra recorded at the open-circuit potential both before and after reduction of anthraquinone and at 0.70 V (Fig. 8b). These spectra clearly show that the spectrum at 0.70 V may be assigned principally to trapped electrons. At the open-circuit potential prior to reduction of anthraquinone, the spectrum of reduced viologen is apparently superimposed on that of trapped electrons. Finally, at the open-circuit potential following reduction of anthraquinone, a significantly enhanced absorbance by both trapped electrons and reduced viologen is observed.

In short, at the open-circuit potential light-induced vectorial electron flow is observed as in Scheme 3. At an applied potential of 0.70 V light-induced vectorial electron flow is, it appears, largely suppressed (Scheme 4). Following application of a negative potential step anthraquinone is reduced and light-induced vectorial electron flow is only to the viologen (Scheme 5). Therefore, depending on the potential applied to the intrinsic substrate, constituted from the heterocomponents of $H(TiO_2)$–SVQ, the function of the constituent heterosupermolecules may be modulated between three states. Further, the modulation state of the constituent heterosupermolecules of $H(TiO_2)$–SVQ may be inferred if the potential applied to the intrinsic substrate is known.

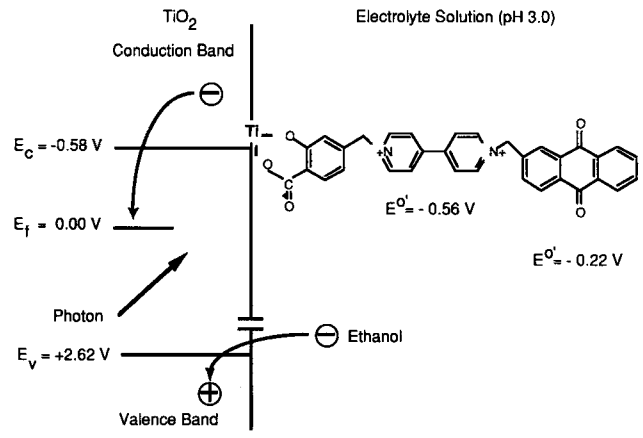

Scheme 4. Suppression of light-induced vectorial electron flow in $H(TiO_2)$–SVQ at an applied potential of 0.70 V.

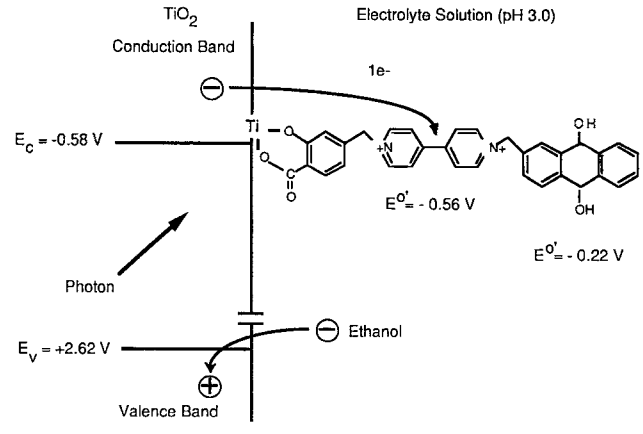

Scheme 5. Light-induced vectorial electron flow in $H(TiO_2)$–SVQ only to the viologen following application of a negative potential step leading to reduction of the anthraquinone moiety.

Concluding Comments

Progress toward realisation of practical devices based on organised assemblies of supermolecules has been slow. Among the reasons for this have been difficulties associated with identifying substrates capable of modulating supramolecular function and providing information concerning modulation state.

Here, we have described preparation of a heterosupramolecular assembly for which the following has been demonstrated: 1) the band-gap excitation of a semiconductor nanocrystallite results in light-induced vectorial electron flow; 2) the electrochemical modulation of the bulk properties of the nanocrystalline semiconductor substrate modulates heterosupramolecular function; and 3) the electrochemical state of the semiconductor substrate provides information about the modulation state of the constituent heterosupermolecules.

Future work will attempt to exploit further the interesting opportunities presented by this and related systems.

Experimental Procedure

Preparation of Transparent Nanocrystallite TiO_2 Substrates: All semiconductor substrates consisted of a 4 μm thick transparent layer of fused TiO_2 particles (12 nm diameter) supported on fluorine doped SnO_2 glass (0.5 μm) supplied by Glastron. Preparation of these substrates has been described in detail elsewhere [25]. Briefly, TiO_2 was prepared by hydrolysis of titanium isopropoxide. The resulting dispersion was concentrated to about 160 g L^{-1} and Carbowax 20000 (40% weight equivalent

0947-6539/96/0204-0426 $ 15.00+.25/0 Chem. Eur. J. 1996, 2, No. 4

of TiO_2) added yielding a white viscous liquid used to form a 4 μm thick layer on conducting glass. After drying in air for one hour, each substrate was fired at 450 °C for 12 h and stored in a vacuum dessicator.

Synthesis of Linked Molecular Components: The linked molecular components in Scheme 1 were prepared as shown in Scheme 6 and characterised by NMR and elemental analysis.

2-Hydroxy-4-methylbenzoic acid (S) was used as supplied by Aldrich.

1-Ethyl-1′-[(4-carboxy-3-hydroxyphenyl)methyl]-4,4′-bipyridinium perchlorate (SV) was prepared as shown in Scheme 6. Detailed reaction conditions, microanalysis and characterisation by NMR have previously been described [7].

1-[(Anthraquinon-2-yl)methyl]-1′-[(4-carboxy-3-hydroxyphenyl)methyl]-4,4′-bipyridinium perchlorate (SVQ) was prepared as shown in Scheme 6. Detailed reaction conditions, microanalysis and characterisation by NMR have previously been described [8].

(*E*)-2-[(3,4-dihydroxyphenyl)ethenyl]anthraquinone (**12**) was prepared as shown in Scheme 6. Calculated for **12** ($C_{22}H_{14}O_4$): C, 77.19; H, 4.09. Found: C, 76.73; H, 4.19. ^{1}H NMR ([D$_6$]DMSO): δ = 6.77–6.79 (d, J = 8.1 Hz, 1H), 6.98–7.02 (dd, J = 1.8 and 8.1 Hz, 1H), 7.10–7.11 (d, J = 1.8 Hz, 1H), 7.10–7.14 (d, J = 16.3 Hz, 1H), 7.34–7.38 (d, J = 16.3, 1H), 7.86–8.21 (m, aromatic, 7H).

1-[(3,4-Dihydroxyphenyl)ethyl]anthraquinone (SQ) was prepared as shown in Scheme 6. Calculated for SQ ($C_{22}H_{16}O_4$): C, 76.74; H, 4.65. Found: C, 76.73; H, 4.65. ^{1}H NMR ([D$_6$]DMSO): δ = 2.80 (m, 2H), 2.98 (m, 2H), 6.46 (d, J = 7.9 Hz, 1H), 6.55 (dd, J = 2.2 and 7.9 Hz, 1H), 6.61 (d, J = 7.9 Hz, 1H), 7.69–8.17 (m, aromatic, 7H), 9.51 (brs, 2H).

Attachment of Linked Molecular Components to Transparent Nanocrystalline TiO_2 Substrates: To attach the linked molecular components in Scheme 1 to the surface of a transparent nanocrystalline TiO_2 substrate, an aqueous solution (typically 2×10^{-3} mol dm^{-3}) of the required compound was prepared. The nanocrystalline substrate was placed in the above solution and adsorption monitored spectroscopically by means of the charge-transfer absorption assigned to chelation of salicylic acid at TiO_2 [11]. The derivatised substrate was washed carefully with distilled deionised water prior to being stored in a darkened desiccator. For all experiments for which results are reported, previously unused samples were employed.

Potential-Dependent Optical Absorption Spectroscopy: A derivatised TiO_2 substrate formed the working electrode (2 cm^2 surface area) of a closed three-electrode single-compartment cell; the counter electrode was platinum and the reference electrode a saturated calomel electrode (SCE). Aqueous electrolyte solutions contained $LiClO_4$ (0.2 mol dm^{-3}) at pH 3.0 (added $HClO_4$). Ethanolic electrolyte solutions contained $LiClO_4$ (0.2 mol dm^{-3}) acidified by addition of 10% by vol. aqueous $HClO_4$ (0.01 mol dm^{-3}) solution. The potential was controlled with a Thompson Electrochem Ministat potentiostat and a Hewlett-Packard 3310B Function Generator. The above cell was incorporated into the sample compartment of a Hewlett-Packard 8452A diode array spectrometer. Difference absorbance spectra, recorded with respect to a background spectrum measured at 0.00 V, are plotted.

Cyclic Voltammetry: All cyclic voltammograms were recorded under the following conditions: The working electrode was a transparent nanocrystalline TiO_2 substrate whose working area was defined by a hardened epoxyresin mask. The counter and reference electrodes were isolated platinum and SCE, respectively. The aqueous electrolyte solution contained $LiClO_4$ (2×10^{-1} mol dm^{-3}) at pH 3.0 (added $HClO_4$) and was deoxygenated by bubbling with argon for 30 min. All scans were recorded at a rate of 0.050 V s^{-1} in 0.005 V steps between 0.200 and −0.800 V. The wait time between scans was 30 s. In each case a background CV was recorded for the substrate prior to derivatisation. This CV was subtracted from that subsequently measured for the substrate following attachment of the linked molecular components.

Band-gap Irradiation of Transparent Nanocrystalline TiO_2 Substrates: To study the effect of band-gap irradiation on potential-dependent absorption spectroscopy measured for a given heterosupramolecular assembly, a derivatised substrate was incorporated as a working electrode in the electrochemical cell described above. The ethanolic electrolyte solution employed contained $LiClO_4$ (0.2 mol dm^{-3}) acidified by addition of 10% by vol. aqueous $HClO_4$ (0.01 mol dm^{-3}) solution and was deoxygenated by bubbling with argon for 30 min. The cell was placed in the sample compartment of a Hewlett-Packard 8452A diode array spectrometer, and the semiconductor substrate irradiated in situ from the conducting glass side with the pulsed output at 355 nm (10 Hz, stated pulse energy) of a Continuum-Surlite Nd:Yag laser. Stated pulse energies are not corrected for reflection losses. The applied potential was as stated, otherwise open-circuit conditions were applied.

To study the effect of band-gap irradiation on the CV measured for a given heterosupramolecular assembly, the derivatised substrate in question was removed from the electrochemical cell, washed carefully with distilled deionised water and placed in an ethanolic electrolyte solution containing $LiClO_4$ (0.2 mol dm^{-3}) acidified by addition of 10% by vol. aqueous $HClO_4$ (0.01 mol dm^{-3}) solution and deoxygenated by bubbling with argon for 30 min. The derivatised substrate was irradiated from the conducting glass side with the pulsed output at 355 nm (10 Hz, stated pulse energy) of a Continuum-Surlite Nd:Yag laser. Stated pulse energies are not corrected for reflection losses. Following irradiation the derivatised substrate was again washed with distilled deionised water and replaced in the electrochemical cell used for CV measurements.

Real-time Transient Absorbance Optical Spectroscopy: Real-time transient optical absorbance measurements were recorded on a spectrometer based on a previously described design [26]. Briefly, the continuous output of a Coherent Ar-ion laser (Innova 70-5) was used to pump a Coherent dye laser (Model 599-01 with Rhodamine 110, Rhodamine 6G and DCM). The dye laser output was split (40/60%) into two beams. One beam (40%) was allowed fall directly incident on one photo diode of a dual diode detector. The second beam (60%) passed through the sample before falling incident on the second photodiode of the detector. The detectors used were United Detector Technology PIN-10D silicon photodiodes protected against scattered 355 nm or 532 nm light by a Melles Griot OG-550 optical cut-on filter. The associated circuitry was configured to generate a d.c. voltage proportional to the difference in intensity of the two beams incident on the dual-diode detector. This

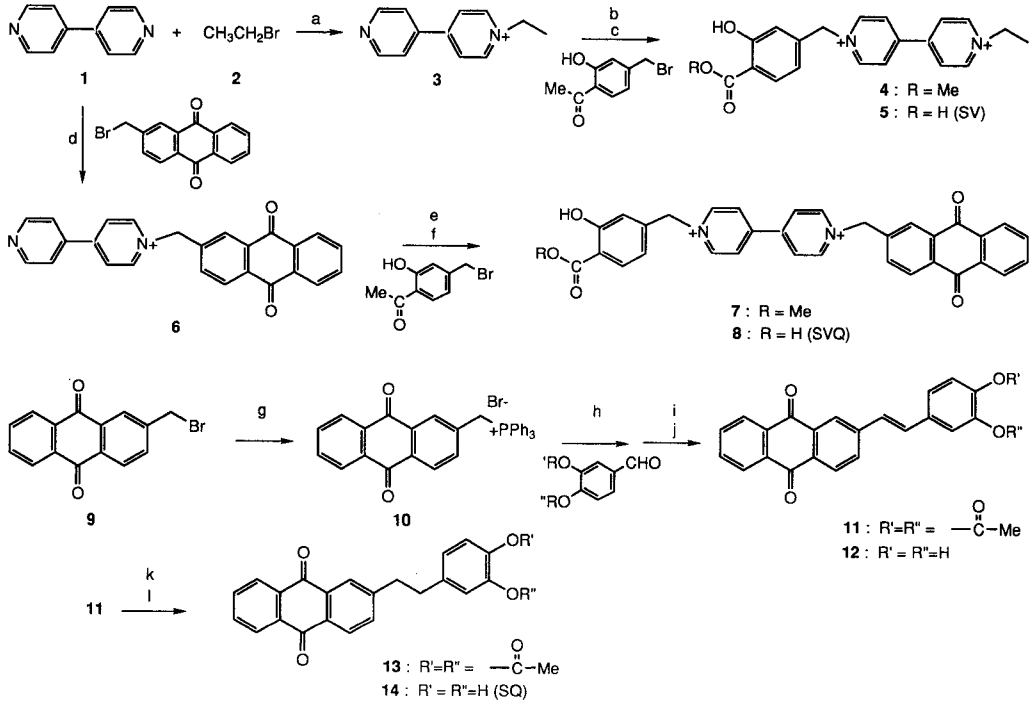

Scheme 6. a) Toluene, 110 °C. b) MeCN, 80 °C. c) $HClO_4$ (1.0 mol dm^{-3}), 100 °C. d) Toluene, 110 °C. e) MeCN, 80 °C. f) $HClO_4$ (1.0 mol dm^{-3}, 50% by vol. in DMSO). g) $(C_6H_5)_3P$, toluene, reflux 3 h. h) NaH, DMSO, 80 °C, 4 h. i) I_2, toluene, reflux, 4 h. j) Methanolic NaOH (1:1 by vol.). k) 10% Pd/C, H_2 at 3 atm. l) Methanolic NaOH (1:1 by vol.).

signal was amplified and digitised by means of a Le Croy 9410 oscilloscope. The sample was excited at right angles to the probe beam with the pulsed output (single-shot or 10 Hz) at 355 nm or 532 nm of a Nd:YAG laser (Continuum-Surlite).

Acknowledgements: This work was supported by a grant from Forbairt (The Irish National Science and Technology Agency). X. M. is supported by a fellowship from the Swiss National Science Foundation.

Received: August 30, 1995 [F200]

[1] V. Balzani, F. Scandola, *Supramolecular Photochemistry*, Ellis Horwood, New York, **1991**, Chapt. 2.
[2] J.-M. Lehn, *Angew. Chem. Int. Ed. Eng.* **1990**, *29*, 1304.
[3] J.-M. Lehn, *Angew. Chem. Int. Ed. Eng.* **1988**, *27*, 89.
[4] G. Ashwell, *Molecular Electronics*, Wiley, New York, **1992**.
[5] J. Hopfield, J. Nelson-Onuchic, D. Beretan, *Science* **1988**, *241*, 817.
[6] Advances in high spatial resolution at the solid–liquid interface are encouraging regarding addressability and have recently been reviewed in detail by A. Bard, H. Abrũna, C. Chidsey, L. Faulkner, S. Feldberg, K. Itaya, M. Majda, O. Melroy, R. Murray, M. Porter, M. Soriaga, H. White, *J. Phys. Chem.* **1993**, *97*, 7147.
[7] X. Marguerettaz, R. O'Neill, D. Fitzmaurice, *J. Am. Chem. Soc.* **1994**, *116*, 2628.
[8] X. Marguerettaz, D. Fitzmaurice, *J. Am. Chem. Soc.* **1994**, *116*, 5017.
[9] G. Rothenberger, D. Fitzmaurice, M. Grätzel, *J. Phys. Chem.* **1992**, *96*, 5983.
[10] H. Frei, D. Fitzmaurice, M. Grätzel, *Langmuir* **1990**, *6*, 198.
[11] J. Moser, S. Punchihewa, P. Infelta, M. Grätzel, *Langmuir* **1991**, *7*, 3012.
[12] W. Siripala, M. Tomkievicz, *J. Electrochem. Soc.* **1982**, *129*, 1240.
[13] C. Hable, R. Crooks, M. Wrighton, *J. Phys. Chem.* **1989**, *93*, 1190.
[14] C. Hable, R. Crooks, J. Valentine, R. Giasson, M. Wrighton, *J. Phys. Chem.* **1993**, *97*, 6060.
[15] O. S. Ksenzhek, S. A. Petrova, S. V. Oleinik, M. V. Kolodyazhnyi, V. Z. Moskovskii, *Elektrokhimiya* **1977**, *13*, 182.
[16] B. Kok, H. Rurainski, O. Owens, *Biochem. Biophys. Acta* **1965**, *109*, 347.
[17] P. Trudinger, *Ananl. Biochem.* **1970**, *36*, 222.
[18] T. Wantanabe, K. Honda, *J. Phys. Chem.* **1982**, *86*, 2617.
[19] E. Hayon, T. Ibata, N. Lichtin, M. Simic, *J. Phys. Chem.* **1972**, *76*, 2072.
[20] G. Callabrese, R. Buchanan, M. Wrighton, *J. Am. Chem. Soc.* **1983**, *105*, 5594.
[21] The band gap in crystalline anatase is taken as 3.2 eV: H. Finklea in *Semiconductor Electrodes* (Ed.: H. Finklea), Elsevier, New York, **1988**, p. 50.
[22] Ethanol has been shown to act as an efficient hole scavenger in a number of studies: H. Finklea in *Semiconductor Electrodes* (Ed.: H. Finklea), Elsevier, New York, **1988**, p. 113.
[23] A.-M. Brun, S. Hubig, M. Rodgers, W. Wade, *J. Phys. Chem.* **1990**, *94*, 3869.
[24] A.-M. Brun, S. Hubig, M. Rodgers, W. Wade, *J. Phys. Chem.* **1992**, *96*, 710.
[25] B. O'Regan, M. Grätzel, *Nature* **1991**, *353*, 737.
[26] D. Fitzmaurice, M. Eschle, H. Frei, J. Moser, *J. Phys. Chem.* **1993**, *97*, 3806.